Published in final edited form as:
J Mol Cell Cardiol. 2007 October ; 43(4): 504–516. doi:10.1016/j.yjmcc.2007.07.001.

Survival and maturation of human embryonic stem cell-derived cardiomyocytes in rat hearts

Wangde Dai[1], **Loren J. Field**[2], **Michael Rubart**[2], **Sean Reuter**[2], **Sharon L. Hale**[1], **Robert Zweigerdt**[3], **Ralph E. Graichen**[3], **Gregory L. Kay**[1], **Aarne J. Jyrala**[1], **Alan Colman**[3], **Bruce P. Davidson**[3], **Martin Pera**[4], and **Robert A. Kloner**[1]

[1]The Heart Institute, Good Samaritan Hospital, University of Southern California, Los Angeles, California 90017-2395.

[2]Wells Center for Pediatric Research, Indiana University School of Medicine, Indianapolis, Indiana, 46202-5225.

[3]ES Cell International Pte Ltd, One-North, 11 Biopolis Way, #05-06 Helios, Singapore 138667.

[4]Center for Stem Cell and Regenerative Medicine, Keck School of Medicine, University of Southern California, Los Angeles, California 90033.

Abstract

Purpose—Human embryonic stem cell (hESC)-derived cardiomyocytes are a promising cell source for cardiac repair. Whether these cells can be transported long distance, survive, and mature in hearts subjected to ischemia/reperfusion with minimal infarction is unknown. Taking advantage of a constitutively GFP-expressing hESC line we investigated whether hESC-derived cardiomyocytes could be shipped and subsequently form grafts when transplanted into the left ventricular wall of athymic nude rats subjected to ischemia/reperfusion with minimal infarction. Co-localization of GFP-epifluorescence and cardiomyocyte specific marker staining was utilized to analyze hESC-derived cardiomyocyte fate in a rat ischemia/reperfused myocardium.

Methods—Differentiated, constitutively green fluorescent protein (GFP) expressing hESCs (HES3-GFP; Envy) containing about 13% cardiomyocytes were differentiated in Singapore, and shipped in culture medium at 4°C to Los Angeles (shipping time ~3 days). The cells were dissociated and a cell suspension (2×10^6 cells for each rat, n=10) or medium (n=10) was injected directly into the myocardium within the ischemic risk area 5 minutes after left coronary artery occlusion in athymic nude rats. After 15 minutes of ischemia the coronary artery was reperfused. The hearts were harvested at various time points later and processed for histology, immunohistochemical staining, and fluorescence microscopy. In order to assess whether the hESC-derived cardiomyocytes might evade immune surveillance, 2×10^6 cells were injected into immune competent Sprague-Dawley rat hearts (n=2), and the hearts were harvested at 4 weeks after cell injection and examined as in the previous procedures.

Results—Even following 3 days of shipping, the hESC-derived cardiomyocytes within embryoid bodies (EBs) showed active and rhythmic contraction after incubation in the presence of 5% CO_2 at 37°C. In the nude rats, following cell implantation, H&E, immunohistochemical staining and GFP epifluorescence demonstrated grafts in 9 out of 10 hearts. Cells that demonstrated GFP epifluorescence also stained positive (co-localized) for the muscle marker alpha-actinin and exhibited cross striations (sarcomeres). Furthermore cells that stained positive for the antibody to GFP (immunohistochemistry) also stained positive for the muscle marker sarcomeric actin and

Address for correspondence: Robert A. Kloner The Heart Institute Good Samaritan Hospital 1225 Wilshire Boulevard Los Angeles, CA 90017 Tel. : 213-977-4050 Fax. : 213-977-4107 Rkloner@goodsam.org.

demonstrated cross striations. At 4 weeks engrafted hESCs expressed connexin 43, suggesting the presence of nascent gap junctions between donor and host cells. No evidence of rejection was observed in nude rats as determined by inspection for lymphocytic infiltrate and/or giant cells. In contrast, hESC-derived cardiomyocytes injected into immune competent Sprague-Dawley rats resulted in an overt lymphocytic infiltrate.

Conclusions—hESCs-derived cardiomyocytes can survive several days of shipping. Grafted cells survived up to 4 weeks after transplantation in hearts of nude rats subjected to ischemia/reperfusion with minimal infarction. They continued to express cardiac muscle markers, exhibit sarcomeric structure, and were well interspersed with the endogenous myocardium. However, hESC-derived cells did not escape immune surveillance in the xenograft setting in that they elicited a rejection phenomenon in immune competent rats.

Keywords

myocardial regeneration; human embryonic stem cell; cardiomyocytes; cell transplantation; immunology

Introduction

Over the past few years, various cell types, such as fetal or neonatal cardiomyocytes, skeletal muscle myoblasts, mesenchymal stem cells, hematopoietic stem cells, adult cardiac resident stem cells, embryonic stem (ES) cells and others, have been used for cell transplantation therapy in the heart [for review see 1,2]. Among these cell types, ES cells are a promising cell source, because of their capability to undergo unlimited expansion in an undifferentiated state and their ability to undergo inducible differentiation into *bona fide* cardiomyocytes in vitro. Human ES cell (hESC) -derived cardiomyocytes have been shown to have the structural and functional properties of early-stage fetal cardiomyocytes [3]. Thus, in theory, hESC could potentially provide an unlimited supply of cardiomyocytes for cell therapy aimed at regenerating functional myocardium.

Although numerous studies have examined the fate and consequences of murine ESC-derived cardiomyocyte transplantation [4], only a limited number of studies examining transplantation of hESC-derived cardiomyocytes have been reported. These studies [5, 6, 7] used hESC-derived cardiomyocytes generated locally or regionally, a situation that would unlikely be the case in a clinical setting. The purpose of the current study was to determine whether hESC-derived cardiomyocytes can be transported over a long distance, and could survive and mature following transplantation into hearts subjected to ischemia/reperfusion with minimal infarction. Another goal of this study was to follow the fate of donor cells in the myocardium by the robust, GFP-epifluorescence signal marking the employed human cell line.

Materials and Methods

The present study was approved by the Institutional Animal Care and Use Committee of Good Samaritan Hospital, and conformed to the “Guide for the Care and Use of Laboratory Animals” (NIH publication No. 85-23, National Academy press, Washington DC, revised 1996). The Association for Assessment and Accreditation of Laboratory Animal Care International accredits Good Samaritan Hospital. Use of hESC was approved by the Western Institutional Review Board.

Culture of hESCs

The hES cell line HES3-GFP (Envy) [8] from ES Cell International, (http://stemcells.nih.gov/research/registry/esci.asp) at passage numbers between 75-125,

displaying a normal karyotype was used. hESCs were seeded onto mitotically inactive (Mitomycin C, 10μg/ml, Sigma) human fibroblast feeder cells CCD-919Sk obtained from ATCC (American Type Culture Collection) (cat# CRL-1826) using KO-DMEM (Dulbecco's Modified Eagle's Medium) with 20% KO-serum replacement, 1% non-essential amino acids, 2mM L-glutamine and antibiotics (penicillin/streptomycin, all Invitrogen). hESCs were subcultured every 7 days by treatment with collagenase IV (1mg/ml, Gibco) followed by mechanical partitioning of individual colonies.

hESC EB formation and GFP flow cytometry

To induce hESC differentiation, cells were washed once with PBS^{+} and treated with collagenase IV (1 mg/ml) for 3-4 min at 37°C. Collagenase was replaced by serum-free medium (DMEM medium supplemented with 1% MEM non-essential amino acids, 2mM L-glutamine, 1× ITS, 0.1mM β-Mercaptoethanol and Penicillin/Streptomycin (all Invitrogen) and culture plates were scored with a 10 μl pipette tip. Cells were scraped off the culture dish using a cell scraper and transferred to a 50 ml tube (Falcon). The cell pellet was resuspended in fresh serum-free medium and an equal volume transferred to ultra low attachment 6 well plates (Costar). After overnight EB formation, the medium was changed to either fresh serum-free or END2 cell-conditioned medium (END2-CM) generated by exposure of serum-free medium to END2 cells [9] for 4-5 days, followed by filtration through a 0.22 μM Millipore filter. END2 is a visceral-endoderm-like mouse embryonal carcinoma cell line derived from P19 cells. Subsequent medium changes were performed every 3 days, over a period of 12 days. EBs were scored for beating 12 days after formation and a value was assigned as a percentage of contractile EBs versus total EBs in a 6 well plate; about 25-30 EBs per well (150-180 EBs per 6 well plate) were usually observed. To test GFP expression either undifferentiated hESC cultures or day 12 EBs were dissociated to single cells using trypsin (Invitrogen), strained through a 40 μm strainer (BD Biosciences) and analyzed on a flow cytometer (GFP signal vs. forward or side scatter; FACS Calibur, BD Biosciences) applying standard methods.

Cardiomyocyte quantification

To determine the cardiomyocyte content, EBs from 3 independent wells of a 6 well plate were pooled and dissociated to single cells using trypsin (Invitrogen). Cells were collected via centrifugation at 2500 rpm for 4 minutes at 4°C. The cell pellet was resuspended in PBS and a cell count performed. 1×10^5 cells were then spun at 500rpm for 5 minutes onto glass slides at low acceleration using a cytospin system (Shandon). Adherent cells were fixed, stained and the total cell number (via DAPI staining of cell nuclei) and the number of alpha myosin heavy chain positive cells (αMHC, MF-20 Ab, Hybridoma Bank, Iowa; 1:200 followed by respective rabbit-anti mouse Cy3-labeled secondary Ab 1:500, Zymed) were counted in at least 3 independent fields of view at 20× magnification with at least 300 nuclei per field; fields were randomly selected in the DAPI channel (Zeiss Axiovert 200M, Zeiss) avoiding bias towards cardiomyocyte content. The percentage of cardiomyocytes compared to the total cell nuclei number was calculated.

Cell shipment and dissociation

Before shipment EBs were combined and aliquots were collected for total cell count, vitality stain (trypan blue exclusion), and cardiomyocyte quantification (cytospin). END2-CM was replaced by serum-free medium and EB-aliquots representing 2×10^6 cells were placed into a T25 flask (Costar), filled with serum-free medium and tightly closed. Flasks were cooled to 4°C, placed in thermal control boxes (Aeris Dynamics Pte LTD) and shipped (shipping time ranged from 48-72 hours). At their destination surplus medium was removed and flasks were placed back in a cell culture incubator in serum-free medium.

Intracellular calcium transient measurements

For the measurements of intracellular calcium transients, EBs were washed free of the culture medium by continuous superfusion with normal Tyrode's solution for 15 minutesat 2 mL/minute, exposed to rhod-2 (10 micromol/L + 0.02 % [wt/vol] Pluronic F127 [Molecular Probes, Eugene, OR] in normal Tyrode's solution) for 20 minutes at room temperature, then returned to superfusion with dye-free solution for 20 minutes at 2 mL/minute before experimentation. For calcium transient recording, the normal Tyrode's solution was supplemented with 50 micromoles/l cytochalasin D to eliminate motion artifacts [10]. EBs in 60-mm dishes were placed on the stage of an upright microscope modified for 2-photon illumination (Zeiss LSM510-Meta; Carl Zeiss, Jena, Germany) and imaged through a 40× 0.8 NA water dipping objective (Achroplan IR; Zeiss). Two-photon illumination was provided by a mode-locked Ti:Sapphire laser (Spectraphysics, Mountain View, CA) tuned to a center wavelength of 810 nm. Pulse duration and pulse repetition rate were 100 fs and 83 MHz, respectively. Emitted light was collected by two photomultipliers fitted with a narrow bandwidth filter for 500 to 550 nm (GFP) and 560 to 650 nm (rhode-2). To induce action potential-evoked calcium transients, EBs were field stimulated via 2 ms square wave pulses with approximately 1.2-fold threshold amplitude. The stimuli were delivered by a programmable stimulator (SD9, Grass-Telefactor) via a pair of platinum wire electrodes. A single line across the entire EB width was repeatedly scanned at a frequency of 325 Hz, and composite line-scan images were constructed by stacking scan lines vertically. Fluorescence signals were digitized at 8-bit resolution and stored on the computer's hard disk for off-line analysis. The experiment was performed at room temperature.

Cell transplantation

EBs were washed twice in PBS^{-} (Gibco) incubated in a diluted trypsin solution (0.05% in PBS^{-}, Gibco) for up to 15 minutes and carefully triturated. Cells were collected via centrifugation at 1200rpm for 5 minutes and resuspended in serum-free injection medium.

Under aseptic conditions, athymic nude rats (Charles River Laboratories, Inc., Wilmington, MA) were anesthetized with intraperitoneal ketamine (75 mg/kg) and xylazine (5 mg/kg), intubated and mechanically ventilated with filtered room air (rate 60 cycles/minute, tidal volume 1 ml per 100 g body weight, Harvard Apparatus Rodent Ventilator, Model 683, South Natick, Mass). The heart was exposed by a left thoracotomy through the 4^{th} intercostal space. The free wall of the left ventricle was exposed after the pericardium was excised. The left anterior descending coronary artery was encircled with a silk suture. The artery was occluded and 5 minutes later cells (2×10^6 cells in 100 μl serum free medium for each rat, n=10) or serum free medium (100 μl, n=10) were injected directly into the risk area with a 28-gauge needle attached to an insulin syringe. Previously we have reported that retention of cells is greater when injected directly into an occluded coronary artery bed compared to injection into a non-occluded coronary artery bed, presumably due to less washout of cells [11]. Each heart received only one injection at one site. The duration of coronary artery occlusion was 15 minutes after which the coronary artery was fully reperfused. The rats were monitored postoperatively and were housed in sterilized cages. Buprenex (0.001mg/100g body weight, twice daily) was given for 2 days as analgesic.

In order to assess whether the hESC might evade immune surveillance, 2×10^6 hESC-derived cardiomyocytes were injected into two immune-competent Sprague-Dawley rat hearts, and the hearts were harvested at 4 weeks after cell injection and examined as the same methods used for nude rats.

Identification of transplanted cells; histological and cytological studies

Rats were anesthetized, and hearts were arrested in diastole by an intravenous injection of 2 milli-equivalents KCl at 1, 2 or 4 weeks after transplantation. The excised hearts were processed for detection of grafted cells by histology, immunohistochemical staining, or fluorescence microscopy and immunofluorescence microscopy.

For Hematoxylin and Eosin (H&E) staining and immunohistochemical staining, hearts were fixed in 10% formalin, embedded in paraffin and sectioned at 5 μm. For GFP epifluorescence and immune staining, hearts were perfusion fixed in paraformaldehyde and cacodylic acid, cryoprotected in 30% sucrose and sectioned as described previously [12]. Immunohistochemical and cytological staining was performed with primary antibody against GFP (1:50, Chemicon), sarcomeric actin (1:75, Dako), myosin light chain-2a (MLC-2a; 1:50, Synaptic Systems), Tropomyosin (1:1000, Sigma), alpha myosin heavy chain (αMHC, MF20, 1:200, Hybridoma Bank, Iowa), alpha-actinin (1:800, Sigma), cytokeratin 8 (Troma1, 1:10, Hybridoma Bank, Iowa) and connexin43 (1:200, Chemicon).

Results

Cultured hESC-derived cardiomyocytes were tested for their ability to form grafts in ischemic myocardium. We utilized a recently developed culture process which gives rise to enhanced cardiomyogenic differentiation. Colonies of hES3-GFP cells were dispersed via collagenase IV digestion and grown in suspension culture in serum free medium conditioned by the visceral endoderm-like cell line END2 [13]. Robust cardiac induction was obtained, with an average of 57.5 ± 7.5 % of the EBs in a plate exhibiting spontaneous contractile activity (see video, Supplemental Data). EBs were gently dissociated via trypsin digestion and trituration [14], and the resulting dispersed cells were either collected (using a cytospin apparatus) for cardiomyocyte quantification or plated onto glass chamber slides for immune cytology. Trypan blue staining revealed 87.5 ± 7.5 % cell vitality following EB dissociation. Immune fluorescence analyses revealed clusters of cardiomyocytes, as evidenced by the presence of alpha actinin immune reactivity in plated cells (Figure 1 A), and alpha myosin heavy chain, tropomyosin, myosin light chain 2a, or cytokeratin 8 immune reactivity in EB sections (Figure 1 B-E). Cytospin based quantification using DAPI nuclear staining to calculate the total cell number, and anti-alpha myosin heavy chain immune reactivity to identify the cell type, revealed that the cardiomyocyte content was 12.5 ± 1.8 % in cultures derived from EBs generated in the presence of END2 conditioned medium.

A high proportion of non-cardiomyocyte cells in differentiated cultures stained positive for cytokeratin 8 (Figure 1 E), an intermediate filament marker expressed in epithelial embryonic and extraembryonic endoderm tissue during development and in trophectoderm as well [15]. Notably, cytokeratin 8 is also expressed in simple epithelia throughout the adult body but the expression in day 12 EBs most likely recapitulates the early expression in embryonic endoderm and trophoectoderm. However, expression of cytokeratin 8 may not infer which cell population this represents. Immune reactivity to cytokeratin 8 and the cardiomyocyte marker myosin light chain 2a on serial EB sections showed the labeling of mutually exclusive cell populations (Figure 1 D-E). Semi-quantitative real time PCR revealed high relative expression levels of the endoderm marker gene Sox17 but faint expression of the ectoderm marker Sox1 (data not shown). These findings indicate that besides cardiac mesoderm predominantly endoderm is formed under our differentiation conditions, in line with previous studies utilizing the END2 cell co-culture system to direct cardiac differentiation of hES [13, 16].

The genetically engineered cell line hES3-GFP (Envy [8]) was employed to provide unambiguous identification of donor cells following transplantation. These cells carry a transgene which utilizes the human beta-actin promoter to drive expression of the green

fluorescent protein (GFP). Undifferentiated hESC3-GFP cells as well as EBs derived thereof exhibit robust GFP expression as evidenced by direct visualization of epi-fluorescence (Figure 1H), anti GFP-specific immune reactivity (Figure 1F and G), and flow cytometric analyses (Figure 2). To determine if hESC-derived cultures could survive shipping, cells were differentiated in vitro for 12 days, at which point beating EBs were readily apparent. The EBs were collected and shipped at 4-8 °C from Singapore to Los Angeles or Indianapolis (up to 72 hour transit time). Rhythmical EB contraction was observed upon arrival following a short incubation at 37°C, 5% CO_2 and the expected presence of cardiomyocytes was evidenced by sarcomeric actin immune reactivity (Figure 1 I). Shipped EBs were loaded in vitro with the calcium sensing dye rhod-2, and electrically evoked changes in rhod-2 fluorescence, indicative of action potential-induced intracellular calcium transients, were readily detected (Figure 3A). Examination of integrated traces obtained from these data (Figure 3B) revealed intracellular calcium transients typical for human cardiomyocytes [17].

The shipped EBs were dispersed via trypsin digestion and the resulting cells were implanted into transiently ischemic myocardium. The animals were euthanized and hearts were harvested and processed for light or fluorescent immune histology at various time points thereafter. Hearts were harvested at 1.5 hours (n=1), 2.5 hours (n=1), 1 week (n=2), 2 weeks (n=3) and 4 weeks (n=3) following cell transplantation. In the control group, hearts were harvested at 0.5 hour (n=1), 1 week (n=3), 2 weeks (n=3) and 4 weeks (n=3) following injection. Initial analyses relied on immune histochemistry with chromogenic secondary antibodies. GFP immune reactivity was readily detected in hearts receiving hESC-derived cells (Figure 4), but not in non-engrafted hearts. Immune fluorescence analyses were performed to further characterize the engrafted hESC-derived cardiomyocytes. Control experiments established co-localization of GFP-immune reactivity (horseradish peroxidase-conjugated secondary antibody) and GFP epi-fluorescence on adjacent sections from hearts harvested 2.5 hours after cell implantation (Figure 5). No signal was observed with non-specific primary anti-body (horseradish peroxidase-conjugated secondary antibody) nor by epi-fluorescence at wavelengths outside of the GFP emission spectra (not shown). Thus, under the conditions employed, GFP epi-fluorescence can reliably be used to track donor hESC-derived cells.

To determine if hESC-derived cardiomyocytes survived in ischemic/reperfused myocardium, adjacent sections were screened for the presence of GFP epi-fluorescence and alpha-actinin immune reactivity at 4 weeks following cell transplantation. Examination of sections at low power revealed the presence of grafts several millimeters in length and up to about 1 millimeter thick (Figure 6). Sections were processed for alpha-actinin immune reactivity using a rhodamine conjugated secondary antibody. Visualiation of the sections at higher power revealed the presence of GFP-expressing donor cells with periodic alpha-actinin staining (Figure 6B shows GFP epi-fluorescence, 6C shows alpha-actinin immune reactivity, and 6D shows a merged image), strongly suggesting that hESC-derived cardiomyocytes were present. Variable levels of sarcomeric organization were apparent, with some donor cardiomyocytes showing only immature sarcomeric structure (Figure 6B-D). However, many other donor cells exhibited intermediate (Figure 6E) or mature (Figure 6F) sarcomeric structure, approaching organization similar to native myocardium. hESC-derived donor cardiomyocytes were frequently observed juxtaposed with the host myocardium (Figure 6G, 7). Immunohistochemical staining showed that clusters of engrafted hESC-derived cardiomyocytes stained positive for the antibody to GFP also stained positive for the muscle marker sarcomeric actin (Figure 8). In the nude rats, following cell implantation, H&E, immunohistochemical staining and GFP epi-fluorescence analyses demonstrated grafts in 9 out of total 10 hearts examined.

Anti-connexin 43 immune fluorescence analyses revealed a punctuate pattern of immune reactivity between donor and host cells at the graft/myocardium border, suggestive of the

presence of gap junctions between donor and host cells (Figure 9). In graft regions with immature sarcomeric structure, connexin 43 immune reactivity was present within the cytoplasm and along the borders of donor cells (Figure 9), reminiscent of the pattern seen in fetal heart tissue. In graft regions with more mature myofiber structure, the pattern of connexin43 immune reactivity appeared more organized, with clusters of signal appearing between bordering cells (Figure 9). At 4 weeks post transplantation, mature intercalated discs were not observed between donor and host cardiomyocytes, nor between donor cardiomyocytes. Approximately 25% of the graft/myocardium border exhibited fibrous tissue. Approximately 50% of the graft/myocardium border exhibited close juxtaposition of donor:host cardiomyocytes, but without direct physical contact. Approximately 25% of the graft/myocardium border exhibited close juxtaposition of donor:host cardiomyocytes as depicted in Figure 9.

Finally, several previous cross-species transplantation studies suggested that ESC-derived cells might evade immune surveillance [18,19,20,21]. To directly test this, hESC-derived cardiomyocyte cultures were injected into immune competent Sprague-Dawley rats. At 4 weeks post-implantation, H&E analyses revealed a central zone of necrotic debris near the injection site (Figure 10 A and B). There were an obvious lymphocytic infiltrate containing foreign body giant cells (Figure 10 C and D). This rejection phenomenon was not observed in the hearts of nude rats which received cell transplantation (Figure 8C).

Discussion

The present study demonstrates that cultured hESC-derived cardiomyocytes can be shipped at 4°C for as long as 3 days with no overt loss in viability, and furthermore that the shipped cells survive for at least 4 weeks following transplantation into the left ventricular wall of athymic nude rats subjected to ischemia/reperfusion with minimal infarction. The preponderance of engrafted cardiomyocytes progressed towards a more mature phenotype as evidenced by their enlargement, acquisition of a cylindrical shape, and the development of well-delineated cross striations typical of sarcomeres. hESC3-GFP-derived cells did not escape immune surveillance in the xenograft setting in that they caused a rejection phenomenon in the immune competent Sprague-Dawley rats that was not observed following engraftment in immuno-compromised animals.

In recent years, cell transplantation has emerged as a novel approach for repairing damaged myocardium. Various types of cells have been employed towards this end, including skeletal muscle myoblasts, adult stem cells, fetal/neonatal cardiomyocytes, and ESC-derived cells [for review see 1,2]. Skeletal muscle myoblasts (one of the first donor cell types used in animal models [22] and in the clinic [23]) have the advantage that an autologous source can be used. Following transplantation, skeletal myoblasts form well-differentiated myotubes; however the nascent myotubes do not form electrical junctions with host myocardium [24,25] and thus are unlikely to participate in a functional syncytium. This latter characteristic may underlie the arrhythmias observed in the initial myoblast clinical trial [23]. In addition, the time needed to process and expand autologous myoblast cultures would make it difficult to deliver them in a timely fashion following myocardial infarction. Although other adult stem cells (as for example, bone marrow derived-stem cells and mesenchymal stem cells) retain the advantage of being autologous in source, their ability to undergo “transdifferentiation” to *bona fide* cardiomyocytes remains controversial [2]. In recent early phase clinical trials with bone marrow cells, results were quite mixed and although small but significant effects were detected in some studies, the reasons for the functional impact on the heart remain unclear [26] and may be related to a paracrine effect rather than true replacement of muscle [27,28,29]. In contrast, fetal and neonatal cardiomyocyte donor cells have the advantages of being able to integrate structurally [30] and functionally [31] into the host heart myocardium, and thus can truly

replace infarcted heart muscle [32,33]. Transplantation of these cells has been shown to increase the thickness of the infarct wall, improve left ventricular stroke volume, decrease LV end-systolic volume and improve LV ejection fraction in a rat model of myocardial infarction [32,33]. However their potential clinical application is limited due to the lack of availability of sufficient numbers of donor cells.

ESC-derived cardiomyocytes circumvent many of limitations encountered with the aforementioned donor cells. It is well established that ESCs from mice can be expanded in an undifferentiated state and then induced to differentiate into cardiomyocytes in vitro. Importantly, recent studies have demonstrated that hESCs retain this property: molecular, immune cytologic, and electrophysiologic studies indicated that human ES cells differentiate in vitro into *bona fide* cardiomyocytes [3,34,35] which terminally differentiate [36] and exhibit properties typical of atrial, ventricular and nodal lineage cells [37,38]. These results are supported by the *in vitro* data presented here (i.e., expression of alpha actinin, alpha myosin heavy chain, tropomyosin, myosin light chain 2a, sarcomeric actin, development of sarcomeric structure, and the presence of spontaneous contractile activity). Importantly, ESC-derived cardiomyocytes can be purified by several different strategies [39,40,41], some of which might facilitate production of these cells at a scale and purity required for clinical application of hESCs, a concept that was recently proven with mouse ESC [42].

Given these attributes, it is not surprising that a number of groups have utilized either mouse [reviewed in [4]] or hESC-derived cardiomyocytes as donor cells in transplantation studies. In the case of hESCs, Kehat and colleagues micro-dissected contracting regions of adherent EBs and injected them into immune suppressed pigs with experimental heart block [5]. Small clusters of hESC-derived cells (identified via anti-human mitochondria immune cytology) survived transplantation and some of the cells exhibited alpha-cardiac actin immune reactivity and a cardiomyocyte morphology. Interestingly, pacing activity originating from the site of cell delivery was observed. Using a similar approach, Xue and colleagues [7] transplanted beating GFP-expressing human EBs into the left ventricle of immune suppressed guinea pig hearts, and observed propagating action potential waves which originated from the site of cell engraftment. Both of these studies suggested electromechanical coupling occurred between the donor and host cells. Laflamme et al [6] transplanted cardiomyocyte-enriched preparations of hESC-derived cells into the left ventricular of athymic rats. It is our understanding that in Laflamme's study that the hESC-derived cells were able to survive overnight shipping. At 4 weeks post-transplantation, the grafts consisted predominantly of cardiomyocytes as evidenced by the expression of cardiac markers including beta-myosin heavy chain, myosin light chain 2v, and atrial natriuretic factor. The hESC-derived cells retained the capacity to proliferate even at 4 weeks post-transplantation. Interestingly, teratomas were not observed at 4 weeks and the noncardiac cells, which were observed at 1 day after implantation, were no longer present in the graft at 4 weeks. The mechanisms of clearance of noncardiac cells from the recipient heart remain unknown.

The results presented here confirm and extend these observations. hES3-GFP-derived cardiomyocytes survived and matured in vivo at 4 weeks after transplantation. Importantly, many donor cardiomyocytes exhibited cross striations following anti-alpha actinin immune staining, indicating well developed sarcomeric structures. Transplanted cells also expressed connexin 43 suggesting the potential for electrical connections to host cells. Although many cells at 4 weeks post-transplantation with GFP epi-fluorescence also exhibited alpha-actinin immune fluorescence signal, the exact percentage of cardiomyocytes was difficult to determine as cross striations were not apparent in all of the cells. Immune reactivity to cytokeratin 8, an endoderm marker that was highly expressed in numerous differentiated hES cells before injection (Figure 1 E), was somewhat variable but noted in GFP epi-flourescence positive areas after injection (data not shown), also indicating that transplanted non-cardiomyocytes might

be present at 4 weeks. However, a high correlation between GFP and sarcomeric actin immune reactivity in adjacent sections processed with HRP-conjugated secondary antibodies (Figure 8) suggests that a preponderance of the GFP-expressing donor cells were cardiomyocytes. It is also of note that the grafts in the present study were generated with live cells shipped from a remote site. Given the complexity of ES cell amplification and differentiation, production of donor hESC-derived cardiomyocytes at a central facility (with the requisite technical expertise in cell culture, cardiomyocyte enrichment and quality control) constitutes a preferred approach for the potential clinical application of these cells. Indeed, a similar approach was employed for recent skeletal myoblast transplantation clinical trials [43,44].

The clinical application of embryonic stem cells for cardiac repair has been significantly hampered by their potential teratoma formation. In one study [45], transplantation of undifferentiated human ES cells in SCID-beige mice gave rise to large teratoma formation by 7 weeks post-delivery, comprised of gut epithelium (endoderm); cartilage, bone, smooth muscle, and striated muscle (mesoderm); and neural epithelium, embryonic ganglia, and stratified squamous epithelium (ectoderm). Nussbaum et al [46] injected undifferentiated mouse ES cells into normal and infarcted hearts in nude or immunocompetent syngeneic mice, and observed formation of teratomas in various conditions in this study. Undifferentiated ES cells were not guided to differentiate into cardiomyocytes in either normal or infarcted hearts. The results suggest that guided differentiation of embryonic stem cells toward cardiomyocytes may be necessary in order to avoid teratomas and to regenerate new myocardium. Kolossov et al [47] injected highly purified (>99%) ES cell-derived cardiomyocytes into the injured heart of syngeneic mice. Long-term engraftment was observed, and no teratoma formation was found in the 4-5 months follow-up. However, whether the cells derived from beating EB might form cardiac teratomas after transplantation remains unknown. In our present study, consistent with Laflamme's study [6], we did not find teratoma formation at 4 weeks. Although there was an absence of microscopic evidence for teratoma formation in our animals at 4 weeks post-cell implantation, suggesting that pluripotency had been lost during EB formation in our experiments, the threat of teratorma formation could still exist because there were still undifferentiated cells in the graft. A long-term large scale study is needed to clarify the fate of these undifferentiated cells.

Collectively, these data suggest that hESC-derived cardiomyocytes are one of the more promising sources of donor cells for cardiac regenerative therapy. Nonetheless numerous obstacles remain. For example, the data presented here clearly demonstrate that hESC-derived cells do not escape immune surveillance in a xenograft. Although this observation is at odds with an earlier study wherein cardiac-committed mouse ES cells were transplanted into infarcted sheep myocardium in the absence of immunosuppression [20], recent data from Swijnenburg et al [48] and Grinnemo et al [49] support our results. The use of autologous ES-like donor cells (as for example, isolated from spermatogonial stem cell cultures [50]) or alternatively the development of novel tolerance approaches [51] might circumvent this problem. An additional (and perhaps more formidable) limitation is the relatively small graft size attained following cardiomyocyte transplantation. Strategies aimed at enhancing donor cell survival and/or post-transplantation proliferation will likely be required to attain transmural grafts of hESC-derived cardiomyocytes [reviewed in [52,53]]. Despite these limitations, the fact that hESC give rise to *bona fide* cardiomyocytes which readily survive transplantation into ischemia/reperfused myocardium with minimal infarction supports the development of these cells for potential therapeutic applications.

Supplementary Material

Refer to Web version on PubMed Central for supplementary material.

Acknowledgments

We gratefully acknowledge grant support from the Los Angeles Thoracic and Cardiovascular Foundation and ES Cell International Pte Ltd for the support of this study. This work was supported in part by NIH grant RO1-HL083126 (to Dr. Field LJ.).

References

1. Wold LE, Dai W, Sesti C, Hale SL, Dow JS, Martin BJ, et al. Stem cell therapy for the heart. Congest Heart Fail 2004;10(6):293–301. [PubMed: 15591844]
2. Dai W, Hale SL, Kloner RA. Stem cell transplantation for the treatment of myocardial infarction. Transplant Immunology 2005;15(2):91–97. [PubMed: 16412954]
3. Kehat I, Kenyagin-Karsenti D, Snir M, Segev H, Amit M, Gepstein A, et al. Human embryonic stem cells can differentiate into myocytes with structural and functional properties of cardiomyocytes. J Clin Invest 2001;108(3):407–14. [PubMed: 11489934]
4. Rubart M, Field LJ. Cardiac repair by ES-derived cells. Handbook of Experimental Pharmacology 2006;174:73–100. [PubMed: 16370325]
5. Kehat I, Khimovich L, Caspi O, Gepstein A, Shofti R, Arbel G, et al. Electromechanical integration of cardiomyocytes derived from human embryonic stem cells. Nat Biotechnol 2004;22(10):1282–9. [PubMed: 15448703]
6. Laflamme MA, Gold J, Xu C, Hassanipour M, Rosler E, Police S, et al. Formation of human myocardium in the rat heart from human embryonic stem cells. Am J Pathol 2005;167(3):663–71. [PubMed: 16127147]
7. Xue T, Cho HC, Akar FG, Tsang SY, Jones SP, Marban E, et al. Functional integration of electrically active cardiac derivatives from genetically engineered human embryonic stem cells with quiescent recipient ventricular cardiomyocytes: insights into the development of cell-based pacemakers. Circulation 2005;111(1):11–20. [PubMed: 15611367]
8. Costa M, Dottori M, Ng E, Hawes SM, Sourris K, Jamshidi P, et al. The hESC line Envy expresses high levels of GFP in all differentiated progeny. Nat Methods 2005;2(4):259–60. [PubMed: 15782217]
9. Rubart M, Wang E, Dunn KW, Field LJ. Two-photon molecular excitation imaging of Ca2+ transients in Langendorff-perfused mouse hearts. Am J Physiol Cell Physiol 2003;284(6):C1654–68. [PubMed: 12584115]
10. Mummery CL, van Achterberg TA, van den Eijnden-van Raaij AJ, van Haaster L, Willemse A, de Laat SW, et al. Visceral-endoderm-like cell lines induce differentiation of murine P19 embryonal carcinoma cells. Differentiation 1991;46(1):51–60. [PubMed: 1710586]
11. Dow J, Simkhovich BZ, Kedes L, Kloner RA. Washout of transplanted cells from the heart: a potential new hurdle for cell transplantation therapy. Cardiovasc Res 2005;67(2):301–7. [PubMed: 15907822]
12. Pasunarthi KBS, Nakajima H, Nakajima HO, Soonpaa MH, Field LJ. Targeted expression of cyclin D2 results in cardiomyocyte cell cycle activation and concomitant regression of myocardial infarct size in transgenic mice. Circ Res 2005;96:110–8. [PubMed: 15576649]
13. Passier R, Oostwaard DW, Snapper J, Kloots J, Hassink RJ, Kuijk E, et al. Increased cardiomyocyte differentiation from human embryonic stem cells in serum-free cultures. Stem Cells 2005;23(6):772–80. [PubMed: 15917473]
14. Zweigerdt R, Burg M, Willbold E, Abts H, Ruediger M. Generation of confluent cardiomyocyte monolayers derived from embryonic stem cells in suspension: a cell source for new therapies and screening strategies. Cytotherapy 2003;5(5):399–413. [PubMed: 14578102]
15. Hesse M, Franz T, Tamai Y, Taketo MM, Magin TM. Targeted deletion of keratins 18 and 19 leads to trophoblast fragility and early embryonic lethality. EMBO J 2000;19(19):5060–70. [PubMed: 11013209]
16. Beqqali A, Kloots J, Ward-van Oostwaard D, Mummery C, Passier R. Genome-wide transcriptional profiling of human embryonic stem cells differentiating to cardiomyocytes. Stem Cells 2006;24(8):1956–67. [PubMed: 16675594]
17. Piacentino V 3rd, Weber CR, Chen X, Weisser-Thomas J, Margulies KB, Bers DM, et al. Cellular basis of abnormal calcium transients of failing human ventricular myocytes. Circ Res 2003;92(6):651–8. [PubMed: 12600875]

18. Fandrich F, Dresske B, Bader M, Schulze M. Embryonic stem cells share immune-privileged features relevant for tolerance induction. J Mol Med 2002;80(6):343–50. [PubMed: 12072909]
19. Li L, Baroja ML, Majumdar A, Chadwick K, Rouleau A, Gallacher L, et al. Human embryonic stem cells possess immune-privileged properties. Stem Cell 2004;22(4):448–56.
20. Menard C, Hagege AA, Agbulut O, Barro M, Morichetti MC, Brasselet C, et al. Transplantation of cardiac-committed mouse embryonic stem cells to infarcted sheep myocardium: a preclinical study. Lancet 2005;366(9490):1005–12. [PubMed: 16168783]
21. Drukker M, Katchman H, Katz G, Even-Tov Friedman S, Shezen E, Hornstein E, et al. Human embryonic stem cells and their differentiated derivatives are less susceptible to immune rejection than adult cells. Stem Cell 2006;24(2):221–9.
22. Koh GY, Klug MG, Soonpaa MH, Field LJ. Differentiation and long-term survival of C2C12 myoblast grafts in heart. J Clin Invest 1993;92(3):1548–54. [PubMed: 8376605]
23. Menasche P, Hagege AA, Vilquin JT, Desnos M, Abergel E, Pouzet B, et al. Autologous skeletal myoblast transplantation for severe postinfarction left ventricular dysfunction. J Am Coll Cardiol 2003;41(7):1078–83. [PubMed: 12679204]
24. Leobon B, Garcin I, Menasche P, Vilquin JT, Audinat E, Charpak S. Myoblasts transplanted into rat infarcted myocardium are functionally isolated from their host. Proc Natl Acad Sci U S A 2003;100 (13):7808–11. [PubMed: 12805561]
25. Rubart M, Soonpaa MH, Nakajima H, Field LJ. Spontaneous and evoked intracellular calcium transients in donor-derived myocytes following intracardiac myoblast transplantation. J Clin Invest 2004;114(6):775–83. [PubMed: 15372101]
26. Rosenzweig A. Cardiac cell therapy – mixed results from mixed cells. N Engl J Med 2006;355:1274–7. [PubMed: 16990391]
27. Dai W, Hale SL, Martin BJ, Kuang JQ, Dow JS, Wold LE, et al. Allogeneic mesenchymal stem cell transplantation in postinfarcted rat myocardium: short- and long-term effects. Circulation 2005;112 (2):214–23. [PubMed: 15998673]
28. Gnecchi M, He H, Noiseux N, Liang OD, Zhang L, Morello F, et al. Evidence supporting paracrine hypothesis for Akt-modified mesenchymal stem cell-mediated cardiac protection and functional improvement. FASEB J 2006;20(6):661–9. [PubMed: 16581974]
29. Ebelt H, Jungblut M, Zhang Y, Kubin T, Kostin S, Technau A, et al. Cellular cardiomyoplasty: improvement of left ventricular function correlates with the release of cardioactive cytokines. Stem Cells 2007;25(1):236–44. [PubMed: 16973829]
30. Soonpaa MH, Koh GY, Klug MG, Field LJ. Formation of nascent intercalated disks between grafted fetal cardiomyocytes and host myocardium. Science 1994;264(5155):98–101. [PubMed: 8140423]
31. Rubart M. Two-photon microscopy of cells and tissue. Circ Res 2004;95(12):1154–66. [PubMed: 15591237]
32. Müller-Ehmsen J, Peterson KL, Kedes L, Whittaker P, Dow JS, Long TI, et al. Rebuilding a damaged heart: long-term survival of transplanted neonatal rat cardiomyocytes after myocardial infarction and effect on cardiac function. Circulation 2002;105(14):1720–6. [PubMed: 11940553]
33. Yao M, Dieterle T, Hale SL, Dow JS, Kedes H, Peterson KL, et al. Long-term outcome of fetal cell transplantation on postinfarction ventricular remodeling and function. J Mol Cell Cardiol 2003;35 (6):661–70. [PubMed: 12788384]
34. Xu C, Police S, Rao N, Carpenter MK. Characterization and enrichment of cardiomyocytes derived from human embryonic stem cells. Circ Res 2002;91(6):501–8. [PubMed: 12242268]
35. Mummery C, Ward-van Oostwaard D, Doevendans P, Spijker R, van den Brink S, Hassink R, et al. Differentiation of human embryonic stem cells to cardiomyocytes: role of coculture with visceral endoderm-like cells. Circulation 2003;107(21):2733–40. [PubMed: 12742992]
36. Snir M, Kehat I, Gepstein A, Coleman R, Itskovitz-Eldor J, Livne E, et al. Assessment of the ultrastructural and proliferative properties of human embryonic stem cell-derived cardiomyocytes. Am J Physiol Heart Circ Physiol 2003;285(6):H2355–63. [PubMed: 14613910]
37. He JQ, Ma Y, Lee Y, Thomson JA, Kamp TJ. Human embryonic stem cells develop into multiple types of cardiac myocytes: action potential characterization. Circ Res 2003;93(1):32–9. [PubMed: 12791707]

38. Satin J, Kehat I, Caspi O, Huber I, Arbel G, Itzhaki I, et al. Mechanism of spontaneous excitability in human embryonic stem cell derived cardiomyocytes. J Physiol 2004;559(Pt 2):479–96. [PubMed: 15243138]
39. Klug MG, Soonpaa MH, Koh GY, Field LJ. Genetically selected cardiomyocytes from differentiating embronic stem cells form stable intracardiac grafts. J Clin Invest 1996;98(1):216–24. [PubMed: 8690796]
40. Muller M, Fleischmann BK, Selbert S, Ji GJ, Endl E, Middeler G, et al. Selection of ventricular-like cardiomyocytes from ES cells in vitro. FASEB J 2000;14(15):2540–8. [PubMed: 11099473]
41. Kattman SJ, Huber TL, Keller GM. Multipotent flk-1+ cardiovascular progenitor cells give rise to the cardiomyocyte, endothelial, and vascular smooth muscle lineages. Dev Cell 2006;11(5):723–32. [PubMed: 17084363]
42. Schroeder M, Niebruegge S, Werner A, Willbold E, Burg M, Ruediger M, et al. Differentiation and lineage selection of mouse embryonic stem cells in a stirred bench scale bioreactor with automated process control. Biotechnol Bioeng 2005;92(7):920–33. [PubMed: 16189818]
43. Pagani FD, DerSimonian H, Zawadzka A, Wetzel K, Edge AS, Jacoby DB, et al. Autologous skeletal myoblasts transplanted to ischemia-damaged myocardium in humans. Histological analysis of cell survival and differentiation. J Am Coll Cardiol 2003;41(5):879–88. [PubMed: 12628737]
44. Dib N, Michler RE, Pagani FD, Wright S, Kereiakes DJ, Lengerich R, et al. Safety and feasibility of autologous myoblast transplantation in patients with ischemic cardiomyopathy: four-year follow-up. Circulation 2005;112(12):1748–55. [PubMed: 16172284]
45. Thomson JA, Itskovitz-Eldor J, Shapiro SS, Waknitz MA, Swiergiel JJ, Marshall VS, et al. Embryonic stem cell lines derived from human blastocysts. Science 1998;282(5391):1145–7. [PubMed: 9804556]
46. Nussbaum J, Minami E, Laflamme MA, Virag JA, Ware CB, Masino A, et al. Transplantation of undifferentiated murine embryonic stem cells in the heart:teratoma formation and immune response. FASEB J 2007;21(7):1345–57. [PubMed: 17284483]
47. Kolossov E, Bostani T, Roell W, Breitbach M, Pillekamp F, Nygren JM, et al. Engraftment of engineered ES cell-derived cardiomyocytes but not BM cells restores contractile function to the infarcted myocardium. J Exp Med 2006;203(10):2315–27. [PubMed: 16954371]
48. Swijnenburg RJ, Tanaka M, Vogel H, Baker J, Kofidis T, Gunawan F, et al. Embryonic stem cell immunogenicity increases upon differentiation after transplantation into ischemic myocardium. Circulation 2005;112(9 Suppl):I166–72. [PubMed: 16159810]
49. Grinnemo KH, Kumagai-Braesch M, Mansson-Broberg A, Skottman H, Hao X, Siddiqui A, et al. Human embryonic stem cells are immunogenic in allogeneic and xenogeneic settings. Reprod Biomed Online 2006;13(5):712–24. [PubMed: 17169186]
50. Guan K, Nayernia K, Maier LS, Wagner S, Dressel R, Lee JH, et al. Pluripotency of spermatogonial stem cells from adult mouse testis. Nature 2006;440(7088):1199–203. [PubMed: 16565704]
51. Strom TB, Field LJ, Ruediger M. Allogeneic stem cells, clinical transplantation and the origins of regenerative medicine. Curr Opin Immunol 2002;14(5):601–5. [PubMed: 12183159]
52. Dowell JD, Rubart M, Pasumarthi KB, Soonpaa MH, Field LJ. Myocyte and myogenic stem cell transplantation in the heart. Cardiovasc Res 2003;58(2):336–50. [PubMed: 12757868]
53. Rubart M, Field LJ. Cardiac regeneration: repopulating the heart. Annu Rev Physiol 2006;68:29–49. [PubMed: 16460265]

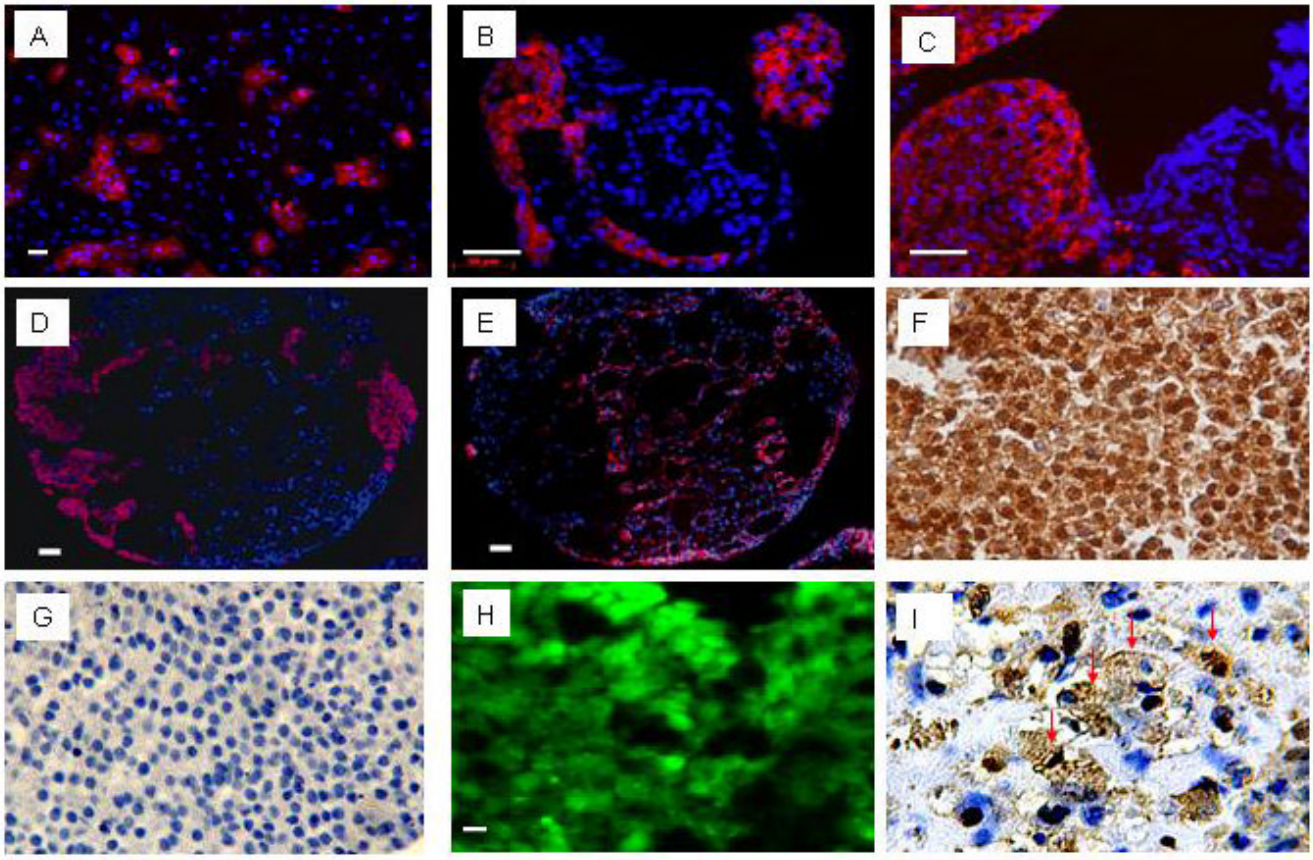

Fig 1.

Characterization of hESC-derived cardiomyocytes. **A-E**: Marker gene expression was demonstrated using rhodamine-conjugated secondary antibodies. Panel A shows anti-alpha-actinin immune reactivity (red) to a monolayer of hESC-derived cells isolated via trypsin-digestions of spontaneously contracting EBs. B-E: Immune staining to EB sections. Panel B shows anti-αMHC immune reactivity, Panel C shows anti-tropomyosin immune reactivity. Serial sections show anti-MLC2a immune reactivity in panel D, and cytoceratin 8 immune reactivity in panel E. Hoechst staining was employed to identify nuclei (blue signal); scale bar, 50 μm. **F**: Immune staining serial sections from a hESC-derived EB with antibody against GFP (HRP-conjugated secondary antibody, signal developed with diaminobenzidine reaction) (400×). **G:** negative control for the anti-GFP staining (i.e., without primary antibody against GFP) (400×). **H**: Epi-fluorescence signal in a hESC-derived EB section (10 μM thick). **I**: Anti-sarcomeric actin immune reactivity in a hESC-derived EB section (HRP-conjugated secondary antibody, signal developed with diaminobenzidine reaction). Many cells are positive to sarcomeric actin (brown) and display cross striations which appear dark brown (marked by red arrows; 600×).

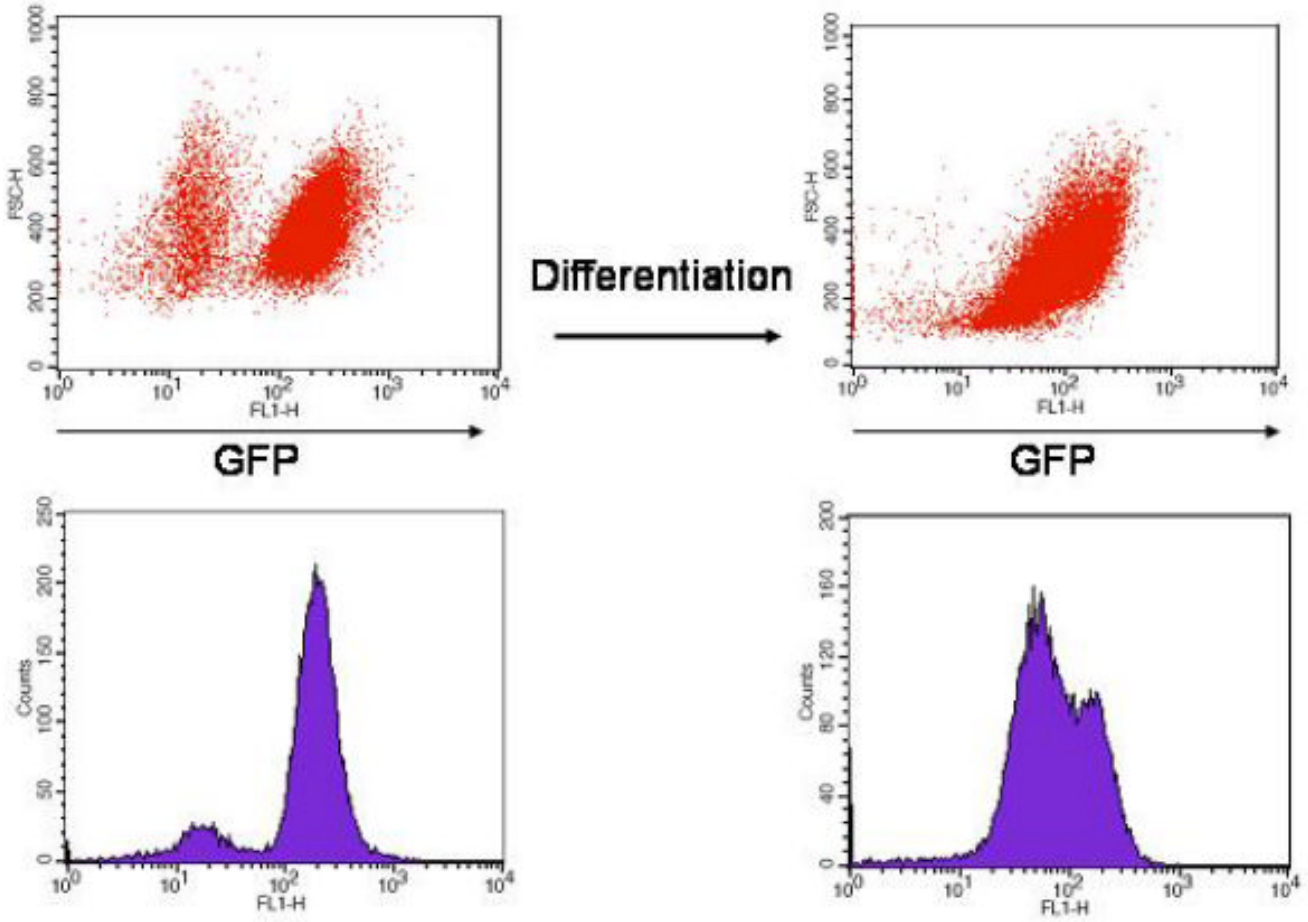

Fig 2.

Flow cytometry analysis of GFP-expression in undifferentiated hES-GFP cells (red dot-plot and blue histogram in the left panel) and day 12 EB-derived cells (right panel). The GFP-negative cell population in the undifferentiated cells likely represents the mitotically inactivated human feeder fibroblasts that are used to co-culture the hES cells and do not carry the GFP transgene. Note that in day 12 EB-derived cells a range of GFP intensity is observed suggesting differing levels of transgenic protein expression.

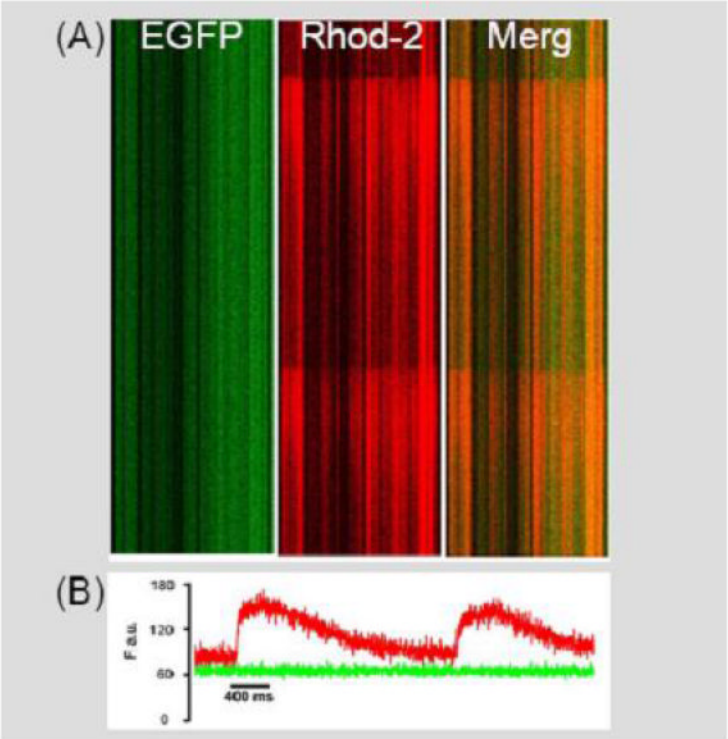

Fig 3.

Shipped hESC-derived EBs exhibit electric field-stimulated intracellular calcium transients. **A:** Stacked line scan images depicting electrically evoked calcium-dependent increases in rhod-2 fluorescence in cultured hESC-derived EBs (y-axis, time; x-axis, position). The left panel shows the EFGP epi-fluorescence signal and the middle panel shows the rhod-2 fluorescence signal. The signals were merged in the right panel. **B:** Spatially integrated traces of the changes in rhod-2 (red) and GFP (green) fluorescence during field stimulation-induced depolarizations in hESC-derived EBs.

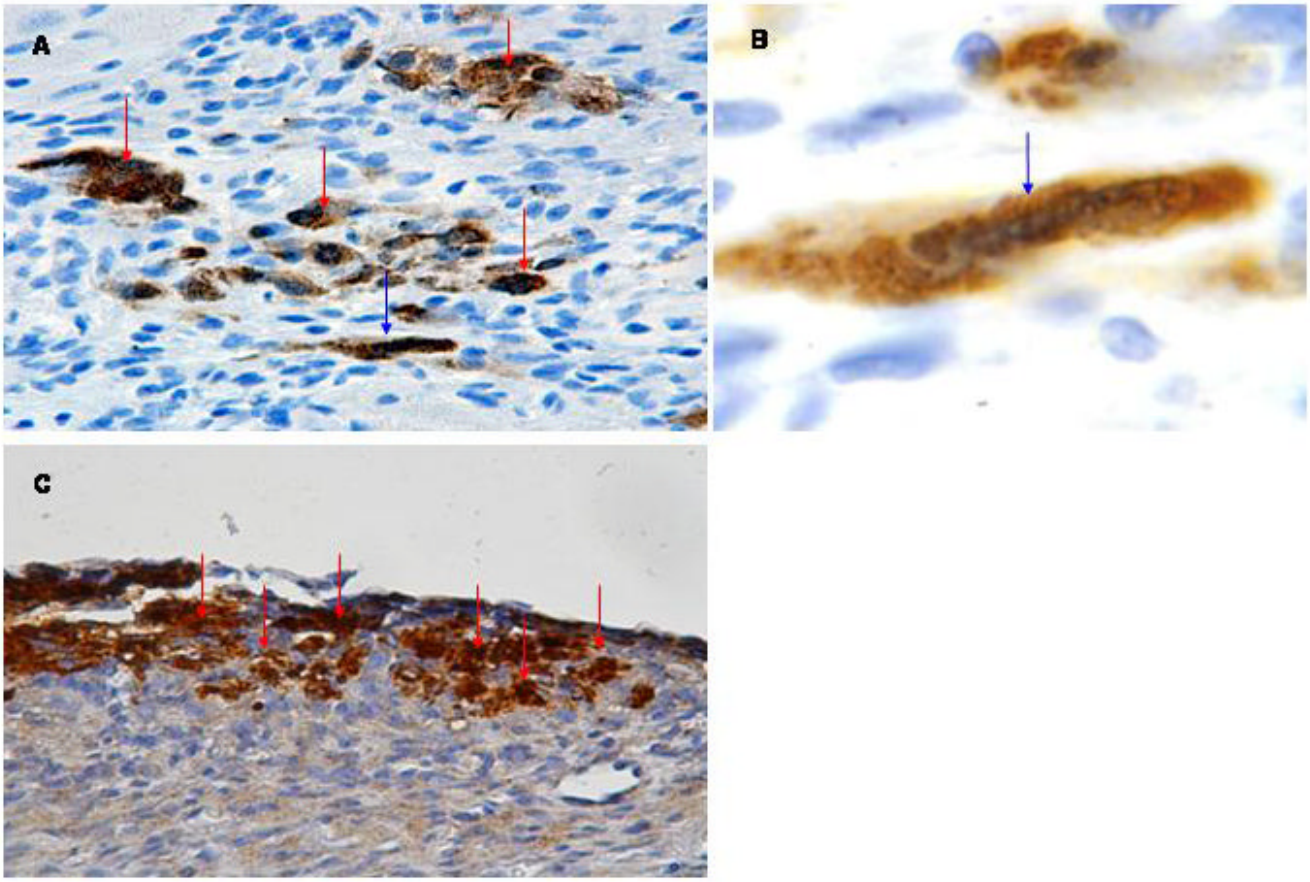

Fig 4.

Detection of hESC-derived cardiomyocytes following transplantation into ischemic myocardium. **A**: Anti-GFP immune reactivity of a heart examined 1 week following cell transplantation (HRP-conjugated secondary antibody, signal developed with diaminobenzidine reaction; see red arrows) (400×). B: Higher magnification of cell indicated by blue arrow in panel A. The cell shows cross striations (blue arrow) and demonstrates a more cylindrical shape (600×). **C**: Anti-GFP immune reactivity of a heart examined 4 weeks following cell transplantation, processed as described in panel A (400×).

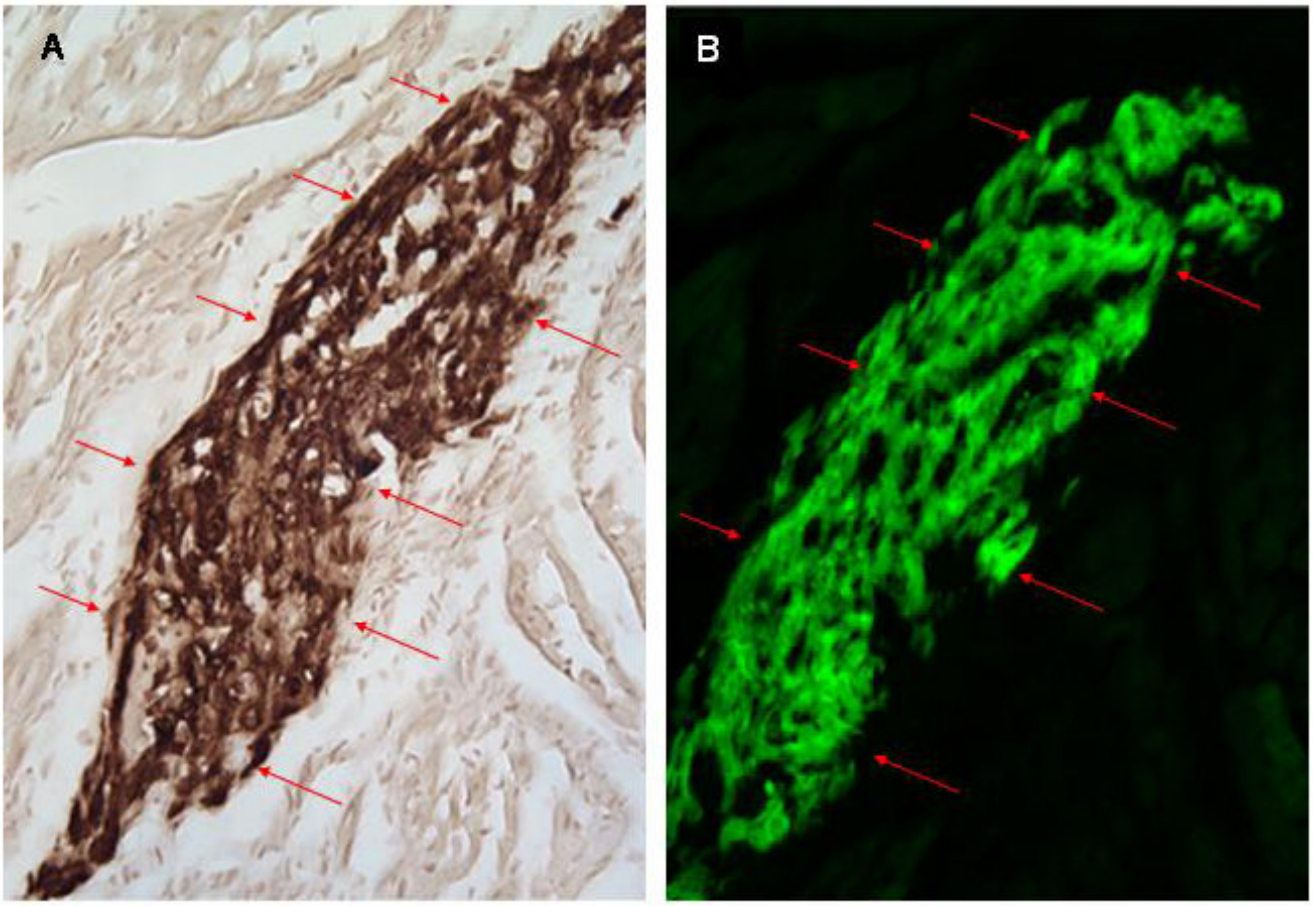

Fig 5.

Co-localization of GFP immune reactivity and epi-fluorescence in serial sections from a heart receiving hESC-derived cardiomyocytes (2.5 hours post-transplantation). **A**: Anti-GFP immune reactivity (HRP-conjugated secondary antibody, signal developed with diaminobenzidine reaction; see red arrows). **B:** GFP epi-fluorescence in an adjacent section to that depicted in panel A.

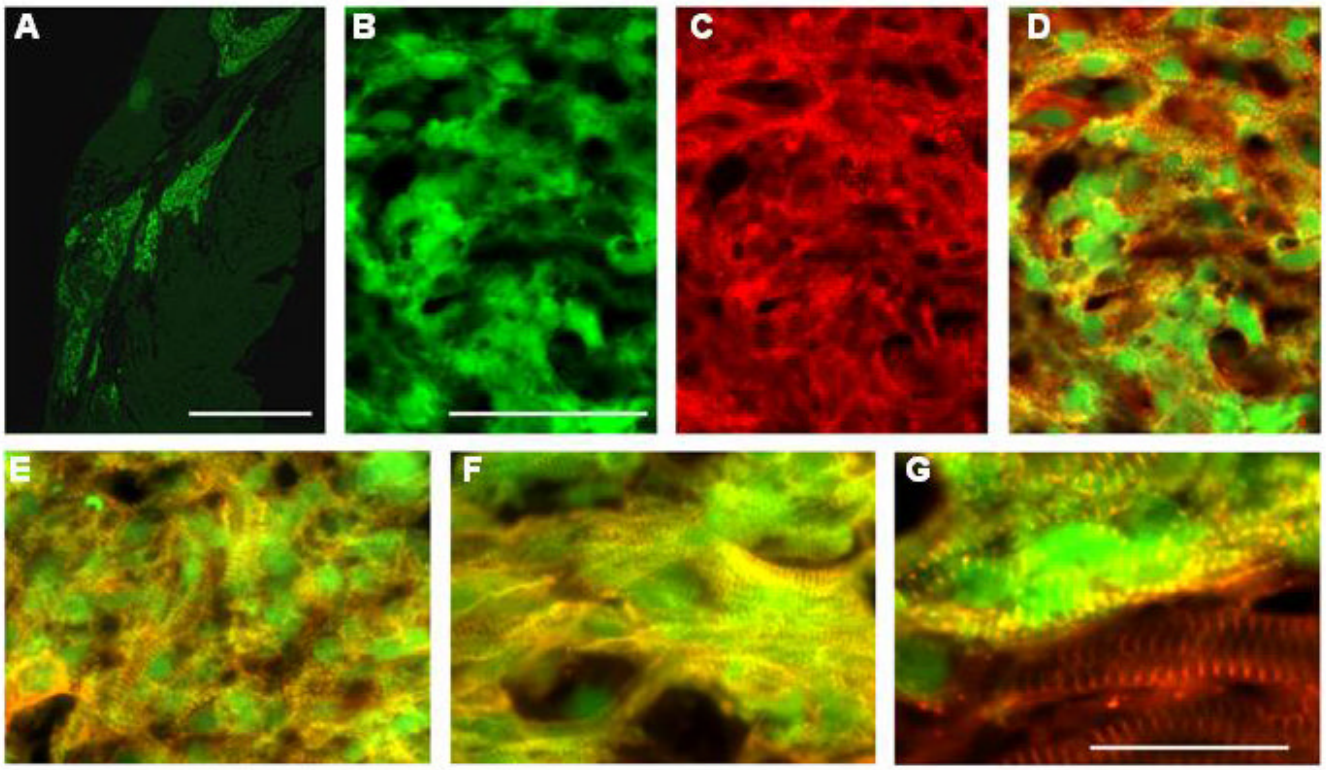

Fig 6.

Analysis of hESC-derived cardiomyocytes 4 weeks after transplantation into ischemic myocardium. **A.** Low power image of GFP epi-fluorescence (green) in a heart engrafted with hESC-derived cardiomyocytes. **B-D.** GFP epi-fluorescence (green; panel B, alpha-actinin immune reactivity (red, rhodamine-conjugated secondary antibody; panel C) and a merged image showing both signals (panel D). Sarcomeric organization in the cardiomyocytes shown is somewhat immature. **E.** Merged image of GFP epi-fluorescence (green) and alpha-actinin immune reactivity (red) of cardiomyocytes with intermediate sarcomeric organization. **F.** Merged image GFP epi-fluorescence (green) and alpha-actinin immune reactivity (red) of cardiomyocytes with a more mature sarcomeric organization. **G.** Merged image GFP epi-fluorescence (green) and alpha-actinin immune reactivity (red) at the graft-host myocardium border. Host cardiomyocytes show alpha-actinin signal only (red, bottom of the panel). Magnification bars correspond to 1 mm (panel A), 50 microns (panels B-F) or 25 microns (panel G).

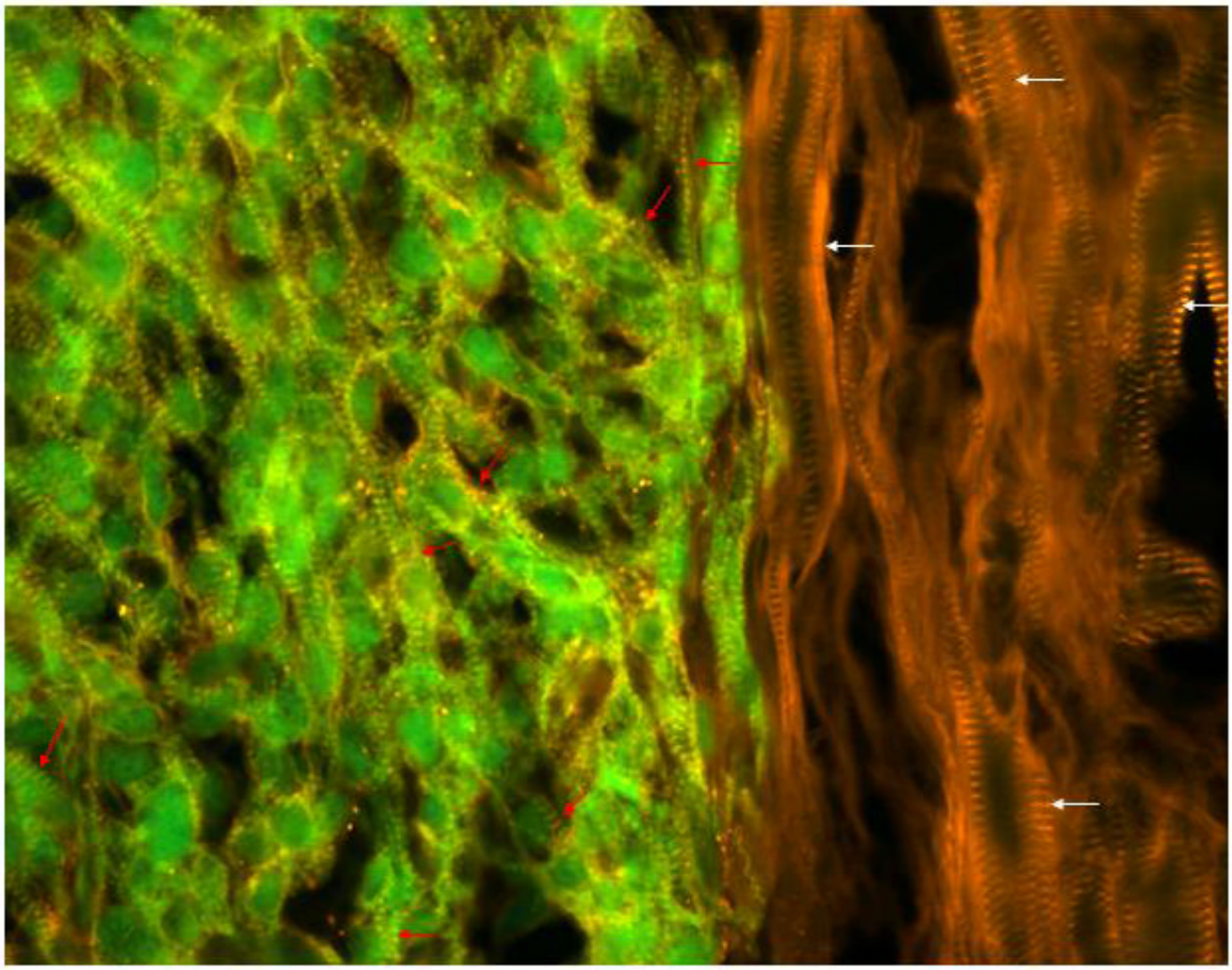

Fig 7.

A merged image with GFP epi-fluorescence (green) and alpha-actinin immune reactivity (red, rhodamine-conjugated secondary antibody) to show the juxtaposition of hESC-derived donor cardiomyocytes and the host myocardium at 4 weeks after transplantation in nude rat. Donor cells are green with yellow color cross striations (red arrows). Host cells show red color cross striations (white arrows). Note that the diameter of transplanted cells (green) is smaller than native cells, and there is some myofiber disarray in the transplant (red arrows).

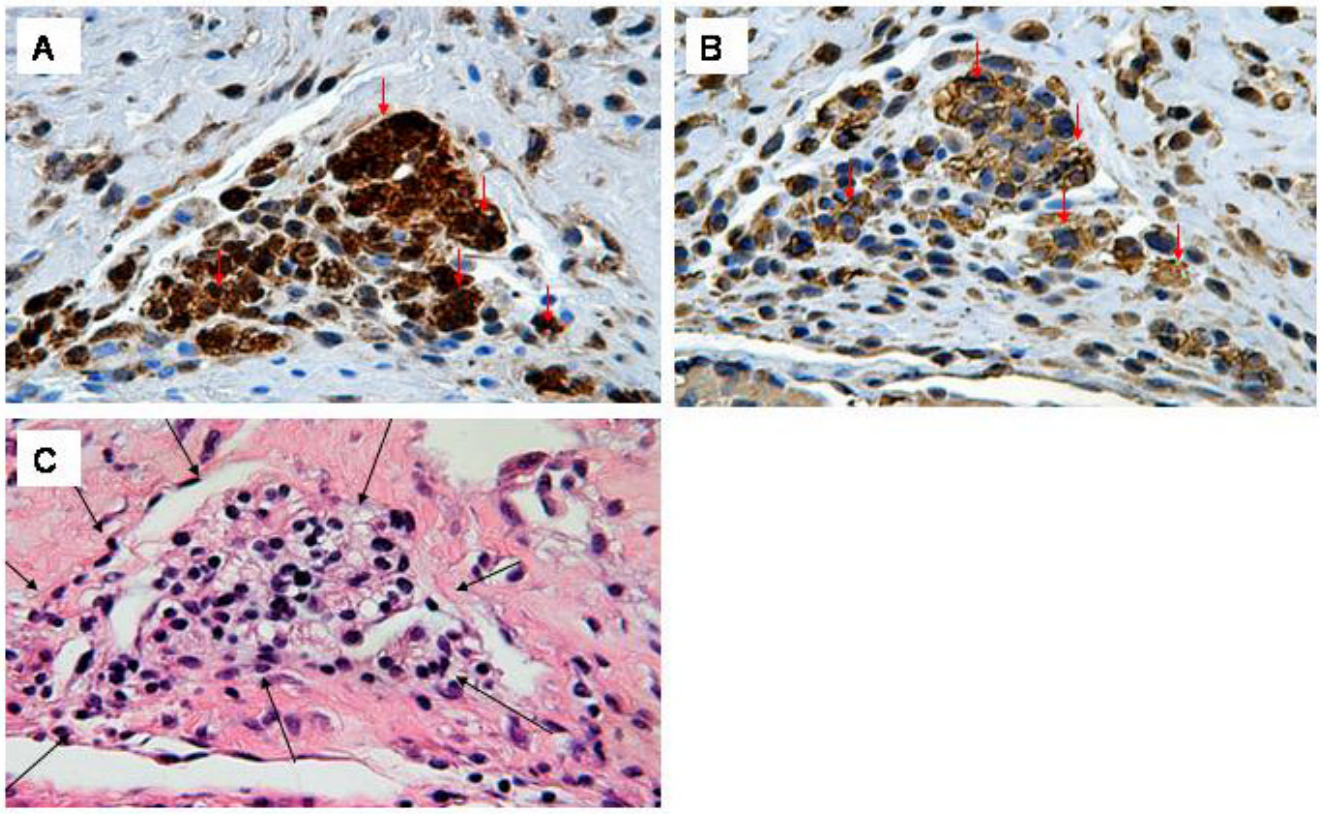

Fig 8.

GFP and sarcomeric actin immune reactivity in hESC-derived cells 4 weeks following transplantation. **A:** Anti-GFP immune reactivity (HRP-conjugated secondary antibody, signal developed with diaminobenzidine reaction) (400×). **B:** Anti-sarcomeric actin immune reactivity on a serial section (HRP-conjugated secondary antibody, signal developed with diaminobenzidine reaction). Note that the preponderance of GFP-expressing hESC-derived cells also stain for sarcomeric actin (arrows) (400×). **C:** H&E staining of an adjacent section; note the absence of any lymphocytic infiltrate around the graft cells (black arrows) (400×).

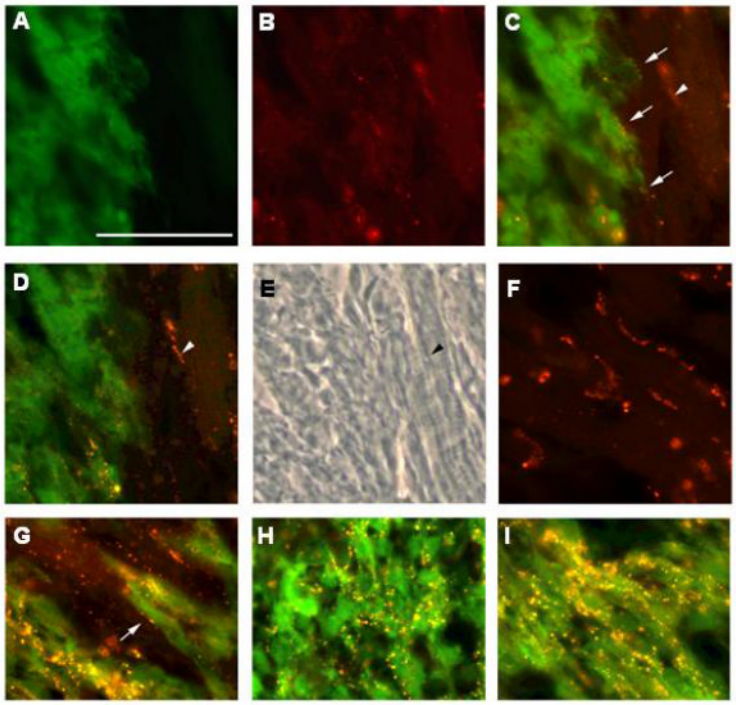

Fig 9.

Engrafted hESC-derived cells express connexin 43 at 4 weeks after transplantation into ischemic myocardium. **A-C.** GFP epi-fluorescence (green; panel A), connexin43 immune reactivity (red, Alexa 555-conjugated secondary antibody; panel B) and a merged image showing both signals (panel C) at the graft/myocardium border. Connexin43 immune reactivity suggestive of the presence of nascent gap junctions can be seen at the junction between a donor and host cells (arrows, panel C; arrowhead indicates a host-host cardiomyocyte junctional complex which is out of the plane of focus). **D.** Same field depicted in Panels A-C, but focused on the host-host cardiomyocyte junctional complex (arrowhead). **E.** Phase contrast image of the same field depicted in Panels A-D; note myofibers present in cells interconnected by the junctional complex (arrowhead). **F.** Connexin43 immune reactivity in remote host myocardium; note the well organized junctional complexes. **G.** Merged image of GFP epi-fluorescence (green) and connexin43 immune reactivity (red) at the graft/myocardium border; arrow points to putative gap junction. **H-I.** Merged image GFP epi-fluorescence (green) and connexin43 immune reactivity (red) of donor cells in graft regions with immature (panel H) and more mature (panel I) myofiber structure. Magnification bar correspond to 50 microns.

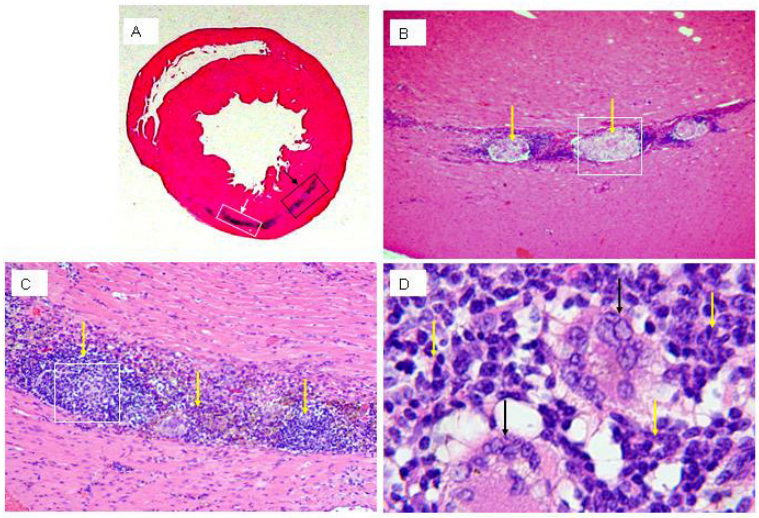

Fig 10.

H&E staining of Sprague-Dawley rat heart at 4 weeks after cell injection. **A**: hematoxylinophilic staining (blue) demarks the area where cells were delivered to the heart. **B**: higher magnification of the boxed area indicted by black arrow in panel A; overt necrosis in the engrafted area surrounded by lymphocytic infiltrate is apparant (yellow arrows, 200×). **C**: higher magnification of the boxed area indicted by white arrow in panel A; the lymphocytic infiltrate in the graft area is apparent (yellow arrows, 200×). **D**: higher magnification of the boxed area in panel **C**; giant cells (black arrows) are surrounded by the lymphocytic infiltrate (yellow arrows) (400×).